Energy Partition in Magnetic Reconnection in Earth's Magnetotail

J. P. Eastwood,[1,*] T. D. Phan,[2] J. F. Drake,[3] M. A. Shay,[4] A. L. Borg,[5] B. Lavraud,[6,7] and M. G. G. T. Taylor[8]

[1]*The Blackett Laboratory, Imperial College London, London SW7 2AZ, United Kingdom*
[2]*Space Sciences Laboratory, University of California, Berkeley, California 94720, USA*
[3]*Department of Physics, Institute for Research in Electronics and Applied Physics, University of Maryland, College Park, Maryland 20742-3511, USA*
[4]*Department of Physics and Astronomy, Bartol Research Institute, University of Delaware, Newark, Delaware 19716, USA*
[5]*Norwegian Defence Research Establishment (FFI), Instituttvn 20, NO-2007 Kjeller, Norway*
[6]*Institut de Recherche en Astrophysique et Planétologie, Université de Toulouse (UPS), 31028 Toulouse Cedex 4, France*
[7]*Centre National de la Recherche Scientifique, UMR 5277 Toulouse, France*
[8]*ESA/ESTEC, 2200 AG Noordwijk, Netherlands*

(Received 15 October 2012; published 31 May 2013)

The partition of energy flux in magnetic reconnection is examined experimentally using Cluster satellite observations of collisionless reconnection in Earth's magnetotail. In this plasma regime, the dominant component of the energy flux is ion enthalpy flux, with smaller contributions from the electron enthalpy and heat flux and the ion kinetic energy flux. However, the Poynting flux is not negligible, and in certain parts of the ion diffusion region the Poynting flux in fact dominates. Evidence for earthward-tailward asymmetry is ascribed to the presence of Earth's dipole fields.

DOI: 10.1103/PhysRevLett.110.225001 PACS numbers: 94.30.cp, 52.35.Vd, 94.30.ct

In plasmas, magnetic reconnection across current sheets releases magnetic energy, heating the plasma and creating jets [1–3]. Since magnetic reconnection lies at the heart of numerous space, solar, astrophysical, and laboratory plasma phenomena, understanding the pathways and mechanisms by which released energy is divided into different forms is an important problem. This is particularly relevant for situations where detailed *in situ* measurements of the plasma and the reconnection region cannot be made, and/or for remote observations which rely on only one component of the plasma (e.g., electron-generated synchrotron radiation).

Scaling arguments and resistive MHD simulations predict that for antiparallel symmetric reconnection configurations in the limit of $\beta_{\mathrm{inflow}} \rightarrow 0$, the outward energy flux is split equally between the kinetic energy flux and the enthalpy flux [4]. However, more generally the enthalpy flux is predicted to exceed the kinetic energy flux [5,6]. Further analysis using hybrid simulations has shown that the ion enthalpy flux may in fact account for ~75% of the outward energy flow ($\beta_{\mathrm{inflow}} = 0.1$) [7]. A common feature of these studies, in addition to neglecting heat fluxes, is that the outward Poynting flux is negligible, in part because scaling arguments lead to the conclusion that the magnetic field in the outflow is small. However, recent particle-in-cell simulations have shown the existence of kinetic Alfvén wave structures in the vicinity of the separatrices, related to ion diffusion region Hall fields that are associated with collisionless reconnection [8,9]. These structures are associated with significantly larger Poynting fluxes in the reconnection outflow than previously expected and extend very long distances from the X line [10].

While the existence of this Poynting flux was detected using *in situ* magnetotail data from the Cluster satellites [10,11], this previous work did not establish the extent to which this Poynting flux was significant in the context of other energy fluxes, nor did it establish the partition of energy flux. Here we address this question by presenting new analysis of the energy flux associated with antiparallel symmetric reconnection in the Earth's magnetotail. We concentrate on the vicinity of the diffusion region, rather than where the jets interact with the dipole field region, finding that whilst the ion enthalpy flux is the largest component of the outflowing energy (even when the jets are fully developed), the Poynting flux is not negligible, and in localized regions of the jet can be dominant.

Figure 1 shows schematically the X-line orientation and ion diffusion region structure in Earth's magnetotail. We use geocentric solar magnetospheric (GSM) coordinates which is generally appropriate for studying magnetotail reconnection [11]. The magnetotail current sheet lies essentially in the x-y GSM plane and so the normal is aligned to the z direction. The x direction points earthward.

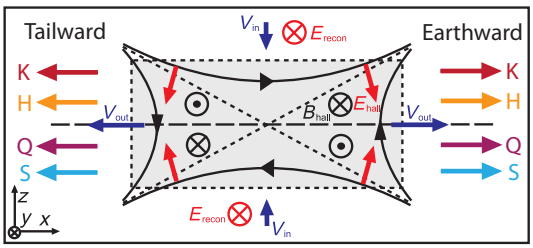

FIG. 1 (color online). The geometry of the reconnection X line in Earth's magnetotail.

The reconnecting magnetic field is B_x, the normal magnetic field is B_z, and the reconnection electric field E_y points in the $+\mathbf{y}$ direction. Reconnection jets point towards and away from the Earth in the $+\mathbf{x}$ and $-\mathbf{x}$ directions, respectively. The Hall magnetic fields are manifested as a quadrupolar signature in the B_y component [3], and the Hall electric fields as a bipolar signature in the E_z component [12].

Based on the energy equation [6], the energy flux is divided into enthalpy flux $\mathbf{H}$, bulk kinetic energy flux $\mathbf{K}$, Poynting flux $\mathbf{S}$, and heat flux $\mathbf{Q}$. We note that previous studies have found that the contribution of any nonthermal component in the magnetotail diffusion region is negligible compared to the ion kinetic energy [13], and so this is neglected in the present calculations. The x components of these fluxes (i.e., along the reconnection outflow) are given by

$$H_{s,x} = (U_s + P_s)v_{x,s} = \frac{\gamma}{\gamma - 1} P_s v_{x,s}, \quad (1)$$

$$K_{x,s} = \left(\frac{1}{2} m_s n_s v_{x,s}^2\right) v_{x,s}, \quad (2)$$

$$S_x = \frac{(\mathbf{E} \times \mathbf{B})_x}{\mu_0} = \frac{E_y B_z - E_z B_y}{\mu_0}. \quad (3)$$

$U_s = P_s/(\gamma - 1)$ is the thermal energy density of species s, P_s is the pressure, γ is the ratio of specific heats (here taken as 5/3), and n_s, m_s and $\mathbf{v_s}$ are the number density, mass, and velocity, respectively. In the single fluid MHD treatment of reconnection, there are no Hall fields. For antiparallel reconnection there is no guidefield B_y and so the "MHD" Poynting flux, associated only with the reconnection electric field E_y and the normal magnetic field B_z is simply $S_x^{\mathrm{MHD}} = E_y B_z/\mu_0$.

We use the collection of 18 antiparallel ion diffusion region encounters made by Cluster between 2001 and 2005 [10,11]. During each encounter, the Cluster satellites [14] flew across the ion diffusion region in the x direction, while taking advantage of natural current sheet flapping to make measurements above and below the current sheet. We use 4s (satellite spin averaged) measurements unless otherwise noted. As such, although the data taken as a whole provides reasonably dense coverage of the ion diffusion region, it is important to always bear in mind how the data are acquired and the limitations this implies [11].

Ion (proton) data is taken from the CIS-CODIF instrument, which is better suited to measuring the proton plasma temperature in the magnetotail [15]. There is no ion plasma data on Cluster 2, which precludes its use in this analysis. Electron data is taken from the PEACE instrument [16] with moments calculated from the ground distributions available at a (variable) lower time resolution. Magnetic and electric field data are taken from the FGM and EFW instruments, respectively, [17,18]. EFW uses wire booms to measure the components of the dc electric field in the spacecraft spin plane and the third component has been reconstructed using the assumption that $\mathbf{E} \cdot \mathbf{B} \sim 0$, i.e., $E_\parallel = 0$, which is expected to be valid down to the ion-scale regions that are the subject of this Letter. The reconstruction requires that $\mathbf{B}$ is not too weak and does not lie near the spin plane; as a result the electric field time series is irregularly sampled. For each event, the proton and electron kinetic energy fluxes ($K_{i,x}$ and $K_{e,x}$), enthalpy fluxes ($H_{i,x}$ and $H_{e,x}$), and heat fluxes ($Q_{i,x}$ and $Q_{e,x}$) were calculated as a function of time, as well as the Poynting flux S_x and the MHD Poynting flux S_x^{MHD}.

Figure 2(a)–2(h) shows the different energy fluxes plotted as a function of $v_{i,x}$, combining all the data points from all events. Since data are plotted on a log scale, positive and negative values are shown in black and blue, respectively. The red lines show the magnitude of the mean flux, where the data have been binned (bin width = 200 km/s). The mean should be taken as negative where a bin contains predominantly blue data points. $v_{i,x}$ is a proxy for the position of the satellite in the x direction relative to the X line, with negative speeds indicating a tailward position and positive speeds an earthward position. Magnetotail flow speeds rarely exceed 1000 km/s [19], and so when the observed flow speed reaches this value, the satellite are sufficiently far from the X line that the flow is likely to have been fully developed. $|K_{i,x}|$ rises with $|v_{i,x}|$, as expected in the context of Eq. (2). $|H_{i,x}|$ also rises with $|v_{i,x}|$; this increase is due to plasma heating, as shown in Fig. 3 where ions in the outflow region (high flow speed) are clearly heated relative to cold ions in the "inflow" region (small flow speed, large magnetic field).

The ion heat flux, $|Q_{i,x}|$, which is expected to be relatively noisy due to low counting statistics and the fact that it is a third-order moment, is negligible. $|S_x|$ is significantly larger than $|S_x^{\mathrm{MHD}}|$. $|K_{e,x}|$, because it scales with species mass, is $\sim 100\times$ smaller than any of the other energy fluxes (note the y-axis scale is different) and can essentially be ignored (hence figures showing $|K_{e,x}|$ are shaded gray). Finally, $|H_{e,x}|$ and $|Q_{e,x}|$ are smaller than $|H_{i,x}|$.

The remainder of Fig. 2 shows the absolute energy fluxes plotted as a function of B_x, which is a proxy for the position above ($B_x > 0$) and below ($B_x < 0$) the current sheet. The middle two rows show only measurements made earthward of the X line ($v_{i,x} > 0$) and the bottom two rows show only measurements made tailward of the X line ($v_{i,x} < 0$) [hence, predominantly positive (black) energy fluxes are seen earthward and negative (blue) tailward]. Both the ion and electron absolute kinetic energy and enthalpy fluxes are higher at the center of the current sheet, and more strongly peaked on the tailward side (but again note that $|K_{e,x}|$, shaded gray, is negligible). However, $|S_x|$ shows an interesting feature: in the earthward direction [Fig. 2(l))] it is bifurcated, with a clear minimum near $B_x = 0$. In the tailward direction [Fig. 2(t)], any bifurcation is less obvious.

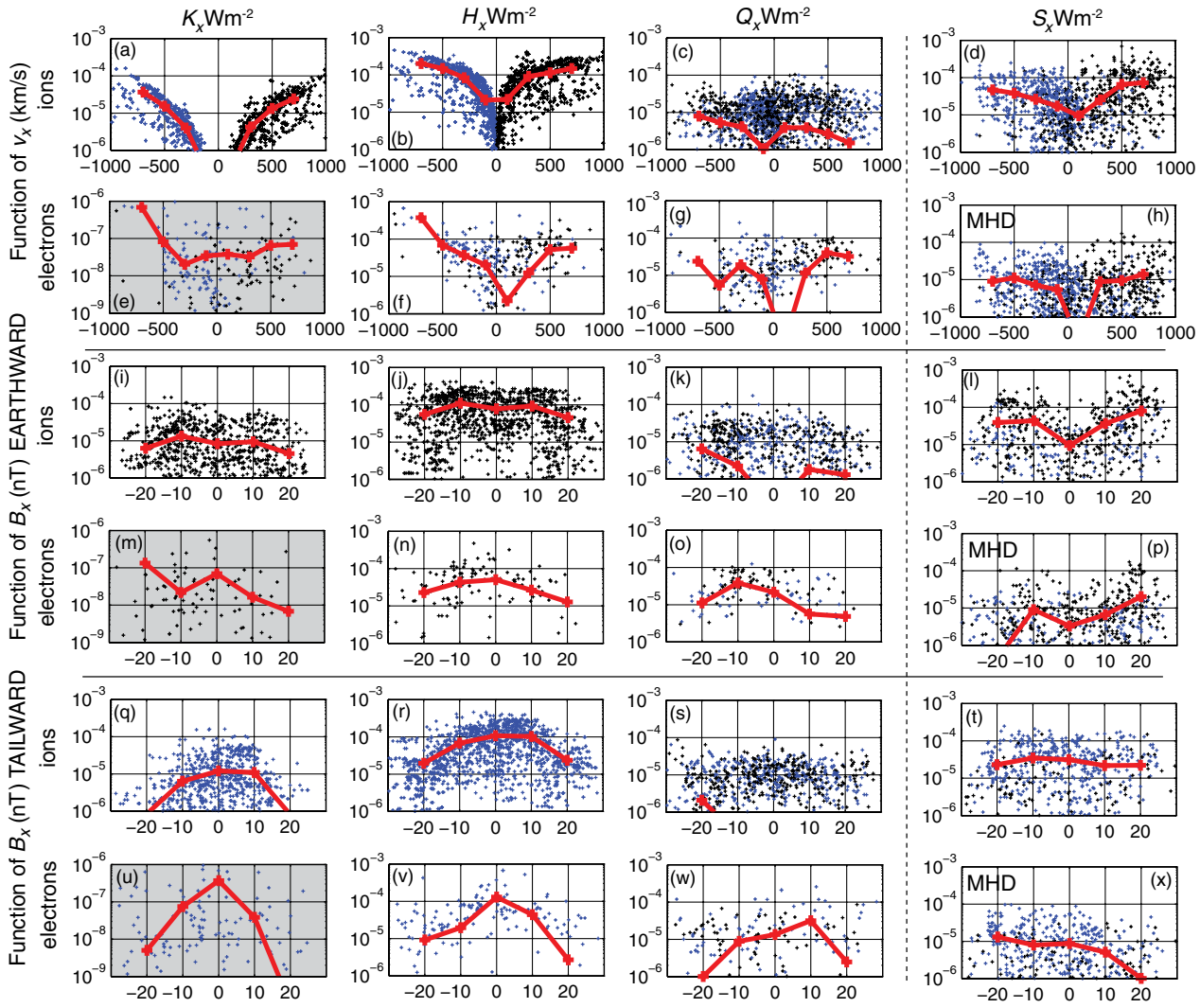

FIG. 2 (color online). (a)–(h) Energy fluxes as a function of outflow speed v_x and as a function of the reconnecting component of the magnetic field B_x in the (i)–(p) earthward and (q)–(x) tailward directions.

Although Figure 2 reveals underlying trends, there is variability from event to event, because each diffusion region encounter was made at different times, with different magnetospheric conditions. To remove this variability, for each encounter, the lobe (inflow) magnetic field strength B_L and maximum ion density (typically at the current sheet) n_c were identified. The data were then scaled as follows [11,20]: $\mathbf{B}' = \mathbf{B}/B_L$, $n' = n/n_c$, $m' = m/m_i$ where m_i is the ion mass, $\mathbf{v}' = \mathbf{v}/v_A(B_L, n_c)$ where v_A is the Alfven speed based on B_L and n_c, and $\mathbf{E}' = \mathbf{E}/(B_L V_A)$. It can thus be shown that the normalized energy flux $E'_F = (\mu_0/V_A B_0^2)E_F$.

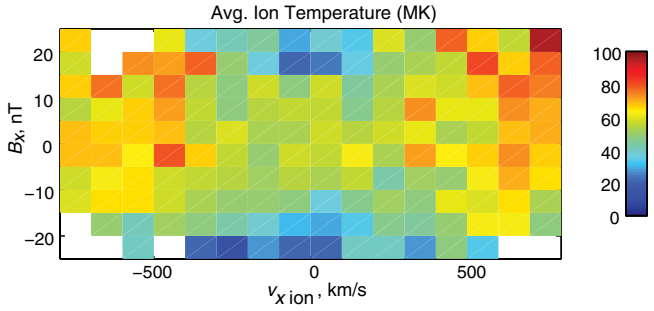

FIG. 3 (color online). Ion temperature as a function of outflow speed v_x and reconnecting component of the magnetic field B_x.

Figure 4 shows the scaled energy fluxes plotted as a function of outflow velocity $v'_{i,x}$ (note that the top two rows of Fig. 2 shows the same data, unscaled). Again, since logarithmic scales are used, positive and negative points are colored black and blue, respectively, and the red lines show the average data (bin width = 0.1). We note that most data points fall in the range $-0.5 < v'_{i,x} < 0.5$, and so only data within this range have been averaged (note that because of fewer data points, the electron data in the range $-0.4 < v'_{i,x} < 0.4$ have been binned). The sub-Alfvénic flow might be expected from slow shocks bounding the symmetric exhaust in the magnetotail [21]. There is

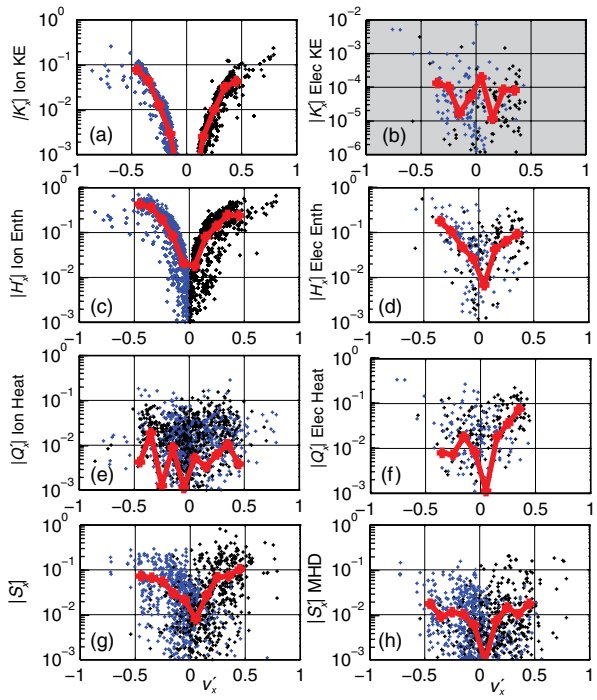

FIG. 4 (color online). Normalized absolute energy fluxes as a function of $v_{i,x}/v_A$.

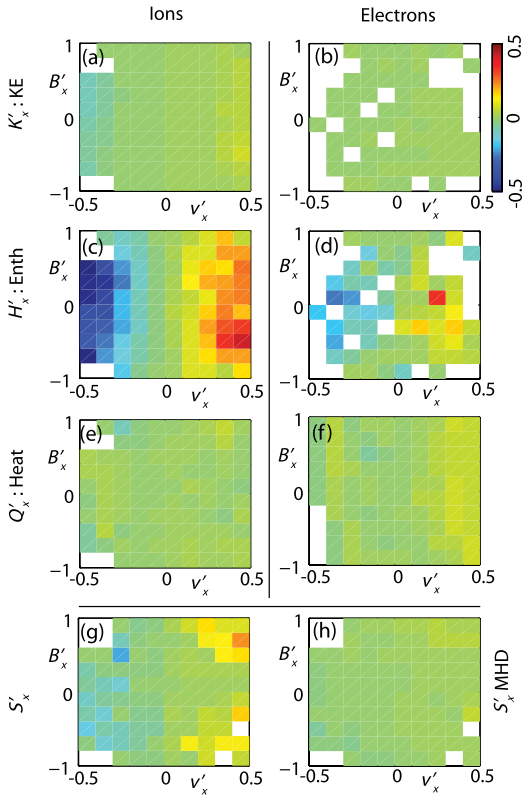

FIG. 5 (color online). Average normalized energy flux as a function of both v'_x and B'_x. Cells with no data are colored white.

less scatter in the scaled ion data; $|H'_{i,x}|$ exceeds $|K'_{i,x}|$, and there is a higher $|H'_{i,x}|$ in the tailward ($v'_{i,x} < 0$) direction. $|Q'_{i,x}|$ is negligible. $|S'_x|$ is an order of magnitude larger than $|S'^{\mathrm{MHD}}_x|$ and as a result is a significant component of the overall energy outflow, being notably comparable to $|K'_{i,x}|$. As before, $|K'_{e,x}|$ is negligible and $|H'_{e,x}|$, while less than $|H'_{i,x}|$, is somewhat larger than $|K'_{i,x}|$. $|Q'_{e,x}|$ appears asymmetric, stronger in the earthward direction. To quantify this, Table I shows the non-negligible normalized energy fluxes for $-0.5 < v'_x < -0.4$ and $0.4 < v'_x < 0.5$.

Figure 4 effectively averages over B'_x, and so some information is lost. Figure 5 bins the energy flux data by both B'_x and $v'_{i,x}$. $H'_{i,x}$ is bigger than $H'_{e,x}$ and $H'_{e,x}$ exceeds $K'_{i,x}$ ($K'_{e,x}$ is clearly unimportant). Figures 5(g) and 5(h) show that Hall effects are crucial to increasing the size of the Poynting flux and making it an important component of the outflow. Figure 5(g) shows the clear bifurcation in S'_x in the earthward flow and that in localized regions it is in fact comparable to $H'_{i,x}$, and certainly greater than $K'_{i,x}$, dominating this region of the jet.

Upstream context.— Because of the difficulty of measuring the cold plasma in the lobes, only characteristic properties can be given. Based on an ion temperature of a few eV, and an average lobe density of 0.047 cm^{-3} [22], then with an inflow field strength ~30 nT, $\beta_{\mathrm{inflow}} \sim 10^{-4}$. Thus a majority of the energy is contained in the magnetic field and the ion thermal velocity in the inflow is much smaller than the outflow velocity.

TABLE I. Average normalized energy fluxes.

$v'^{\,a}_{i,x}$	$K'_{i,x}$	$H'_{i,x}$	$H'_{e,x}$	$Q'_{e,x}$	S'_x
0.45	0.04	0.24	0.09	0.09	0.10
−0.45	−0.08	−0.43	−0.18	−0.01	−0.07

[a]$H'_{e,x}$ and $Q'_{e,x}$ calculated for $\pm 0.35 v'_{i,x}$.

In summary, we have examined the energy fluxes in reconnection jets associated with antiparallel symmetric magnetic reconnection in Earth's magnetotail. The energy flux is dominated by ion enthalpy, with contributions from the electron enthalpy and heat flux and ion kinetic energy flux. The electron kinetic energy and ion heat flux are negligible. The Poynting flux is not negligible, as might be otherwise assumed from simple MHD calculations. The presence of Hall fields increases its value (averaged across the width of the jet) by an order of magnitude to make it comparable with the ion kinetic energy flux. In fact, the Poynting flux is structured across the earthward jet such that in certain regions it may be the dominant component. The differences between the earthward and tailward structuring of the Poynting flux, and the increased energy release on the tailward side may be due to the presence of an obstacle (Earth's dipole field) downstream of the earthward jet and the overall configuration it enforces [6]. Further work is still required to understand the role of plasma β (in particular, distant tail observations where β is lower may indicate a different partition of energy

[13]), asymmetries and/or guide fields (which change the structure of the Hall fields [20]).

This work received support from the STFC grant ST/G00725X/1 at ICL and was partly funded by NASA grant NNX08AO83G at UCB. This work made use of the Cluster Active Archive.

*jonathan.eastwood@imperial.ac.uk

[1] M. Yamada, Phys. Plasmas **14**, 058102 (2007).
[2] V. M. Vasyliunas, Rev. Geophys. **13**, 303 (1975).
[3] B. U. O. Sonnerup, *Magnetic Field Reconnection* (North-Holland, Amsterdam, 1979), p. 47.
[4] E. Priest and T. Forbes, *Magnetic Reconnection* (Cambridge University Press, Cambridge, England, 2000).
[5] J. Birn, J. E. Borovsky, M. Hesse, and K. Schindler, Phys. Plasmas **17**, 052108 (2010).
[6] J. Birn and M. Hesse, Ann. Geophys. **23**, 3365 (2005).
[7] N. Aunai, G. Belmont, and R. Smets, Phys. Plasmas **18**, 122901 (2011).
[8] M. E. Mandt, R. E. Denton, and J. F. Drake, Geophys. Res. Lett. **21**, 73 (1994).
[9] B. N. Rogers, R. E. Denton, and J. F. Drake, J. Geophys. Res. **108**, 1111 (2003).
[10] M. A. Shay, J. F. Drake, J. P. Eastwood, and T. D. Phan, Phys. Rev. Lett. **107**, 065001 (2011).
[11] J. P. Eastwood, T. D. Phan, M. Øieroset, and M. A. Shay, J. Geophys. Res. **115**, A08215 (2010).
[12] M. A. Shay, J. F. Drake, R. E. Denton, and D. Biskamp, J. Geophys. Res. **103**, 9165 (1998).
[13] M. Øieroset, R. P. Lin, T. D. Phan, D. E. Larson, and S. D. Bale, Phys. Rev. Lett. **89**, 195001 (2002).
[14] C. P. Escoubet, M. Fehringer, and M. L. Goldstein, Ann. Geophys. **19**, 1197 (2001).
[15] H. Rème *et al.*, Ann. Geophys. **19**, 1303 (2001).
[16] A. D. Johnstone *et al.*, Space Sci. Rev. **79**, 351 (1997).
[17] A. Balogh *et al.*, Ann. Geophys. **19**, 1207 (2001).
[18] G. Gustafsson *et al.*, Ann. Geophys. **19**, 1219 (2001).
[19] W. Baumjohann, G. Paschmann, and H. Lühr, J. Geophys. Res. **95**, 3801 (1990).
[20] J. P. Eastwood, M. A. Shay, T. D. Phan, and M. Øieroset, Phys. Rev. Lett. **104**, 205001 (2010).
[21] Y.-H. Liu, J. F. Drake, and M. Swisdak, Phys. Plasmas **19**, 022110 (2012).
[22] K. R. Svenes, B. Lybekk, A. Pedersen, and S. Haaland, Ann. Geophys. **26**, 2845 (2008).